Title
Cardiovascular MR imaging after surgical correction of tetralogy of Fallot: approach based on understanding of surgical procedures.

Journal
Radiographics : a review publication of the Radiological Society of North America, Inc, 33(4)

ISSN
0271-5333

Authors
Ordovas, Karen G
Muzzarelli, Stefano
Hope, Michael D
et al.

Publication Date
2013-07-01

DOI
10.1148/rg.334115084

Peer reviewed

TEACHING POINTS
See last page

Cardiovascular MR Imaging after Surgical Correction of Tetralogy of Fallot: Approach Based on Understanding of Surgical Procedures[1]

Karen G. Ordovas, MD, MAS • Stefano Muzzarelli, MD • Michael D. Hope, MD • David M. Naeger, MD • Tom Karl, MD • Gautham P. Reddy, MD, MPH • Edson Marchiori, MD, PhD • Charles B. Higgins, MD

Tetralogy of Fallot (TOF) is one of the most common congenital heart diseases for which patients are referred for postoperative magnetic resonance (MR) imaging evaluation. The most common surgical procedures for TOF repair include infundibulectomy, transannular pulmonary artery patch repair, and right ventricle–pulmonary artery conduit placement. In the past few decades, surgery has proved successful, but most patients require repeat imaging throughout their lives. MR imaging is now frequently used for morphologic and functional evaluation after TOF repair. The most common late postoperative sequelae and residual lesions include right ventricular outflow tract aneurysm and dyskinesis, conduit failure, pulmonary regurgitation, tricuspid regurgitation, right ventricular failure, residual main and branch pulmonary artery stenosis, branch pulmonary artery aneurysm, left pulmonary artery kinking, and residual or recurrent ventricular septal defect. The imaging approach for the evaluation of patients with repaired TOF should be guided by the surgical procedure used and the complications that are expected. Knowledge of the most common postoperative problems and their cardiovascular MR imaging appearances is essential for good radiology practice in this clinical setting.

SA-CME

See www.rsna.org/education/search/RG

LEARNING OBJECTIVES FOR TEST 4

After completing this journal-based SA-CME activity, participants will be able to:

- Describe the expected cardiovascular MR imaging appearance of the heart following the three most common surgical methods for correction of RVOT lesions in tetralogy of Fallot.
- Discuss anatomic and physiologic complications that occur late after repair of tetralogy of Fallot.
- List the cardiovascular MR imaging methods for functional evaluation of the severity of these complications.

Abbreviations: DIR-SE = double-inversion-recovery spin-echo, RVOT = right ventricular outflow tract, SSFP = steady-state free precession, TOF = tetralogy of Fallot, VEC = velocity-encoded cine, VSD = ventricular septal defect

RadioGraphics 2013; 33:1037–1052 • **Published online** 10.1148/rg.334115084 • **Content Codes:** CA CH MR PD

[1]From the Department of Radiology, University Hospital of California, Box 0628, 505 Parnassus Ave, Room L-325A, San Francisco, CA 94143-0252 (K.G.O., S.M., M.D.H., D.M.N., G.P.R., C.B.H.); Queensland Pediatric Cardiac Services, Mater Children's Hospital, Brisbane, Australia (T.K.); and Rio de Janeiro Federal University, Rio de Janeiro, Brazil (E.M.). Recipient of a Certificate of Merit award for an education exhibit at the 2005 RSNA Annual Meeting. Received April 13, 2011; revision requested July 11; final revision received April 30, 2012; accepted June 5. For this journal-based SA-CME activity, the authors K.G.O., S.M., and C.B.H. have disclosed financial relationships (see p 1051); all other authors, the editor, and reviewers have no relevant relationships to disclose. **Address correspondence to** K.G.O. (e-mail: *Karen.ordovas@ucsf.edu*).

See also the article by Ahmed et al (pp 1023–1036) in this issue.

Introduction

Approximately 10% of patients with surgically corrected tetralogy of Fallot (TOF) will develop late complications for which they may need reintervention (1,2). Early detection and treatment of postoperative complications are important to prevent progressive loss of right ventricular function with consequent impairment of exercise capacity and increased risk of fatal arrhythmias (3–6). Cardiovascular magnetic resonance (MR) imaging has emerged as an important imaging modality for the follow-up of patients with complex congenital heart disease, allowing noninvasive, detailed anatomic and functional evaluation without the use of iodinated contrast agents or exposure to ionizing radiation (7–13). In addition, cardiovascular MR imaging provides prognostic information and aids in the decision-making process regarding replacement of a dysfunctional pulmonary valve.

Teaching Point

In this article, we demonstrate the expected cardiovascular MR imaging appearance of the heart following each of the three most common surgical methods for correction of the right ventricular outflow tract (RVOT) lesions in TOF: infundibulectomy, transannular pulmonary artery patch repair, and right ventricle–pulmonary artery conduit placement. In addition, we discuss the appearance of anatomic and physiologic complications late after TOF repair, cardiovascular MR sequences used in the functional evaluation of the severity of these complications, and the scientific evidence supporting the role of MR imaging in guiding clinical decisions concerning repeat surgery and follow-up.

Expected Cardiovascular MR Imaging Appearance of the Heart after Surgical Correction of TOF

The main steps in surgical correction of TOF involve closure of the ventricular septal defect (VSD) and augmentation of the RVOT. The most common surgical methods used for the latter step are *(a)* RVOT muscle resection (infundibulectomy), *(b)* transannular patch repair, and *(c)* right ventricle–pulmonary artery conduit placement. The method for closure of the VSD does not vary significantly with the RVOT augmentation method selected. Closure of the VSD relies on placement of a pericardial or Dacron (DuPont, Wilmington, Del) patch from the edge of the VSD to the aortic annulus, which closes the defect and realigns the aorta with the left ventricular outflow tract.

RVOT muscle resection, or infundibulectomy, is the method of choice for patients with mild to moderate muscular RVOT obstruction and an adequate pulmonary valve annulus. It consists of resection of the hypertrophic myocardium, usually through a longitudinal incision in the right atrium and proximal pulmonary artery (Fig 1). The pulmonary

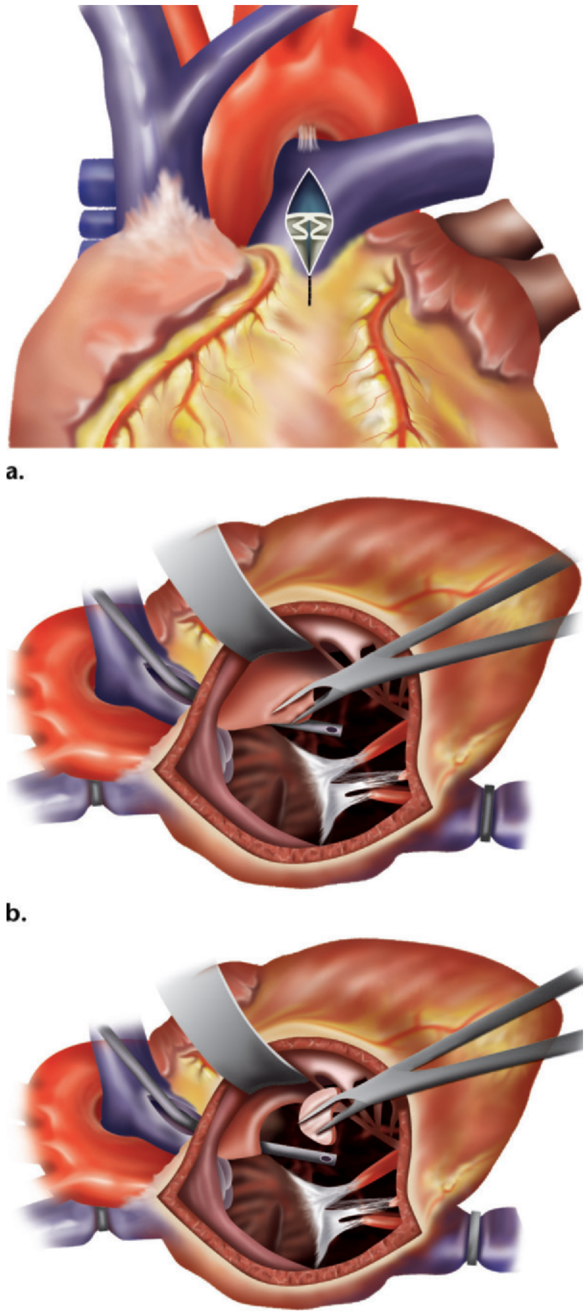

a. b. c.

Figure 1. RVOT muscle resection with a transatrial-transpulmonary approach. **(a)** Drawing illustrates an anterior surgical incision in the main pulmonary artery, sparing the valvular annulus. This incision is performed to allow surgical instrumentation of the RVOT. **(b)** Drawing illustrates an incision in the right atrial wall, with exposure of the RVOT across the tricuspid valve. **(c)** Drawing illustrates resection of the RVOT muscle tissue. (Fig 1 courtesy of Joanna Culley, Haslemere, Surrey, England.)

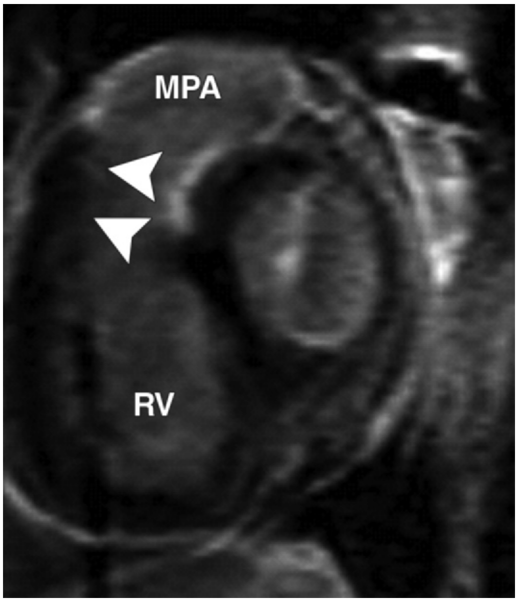

Figure 2. Parasagittal delayed gadolinium-based contrast-enhanced inversion-recovery image shows no evidence of myocardial fibrosis (arrowheads). *MPA* = main pulmonary artery, *RV* = right ventricle.

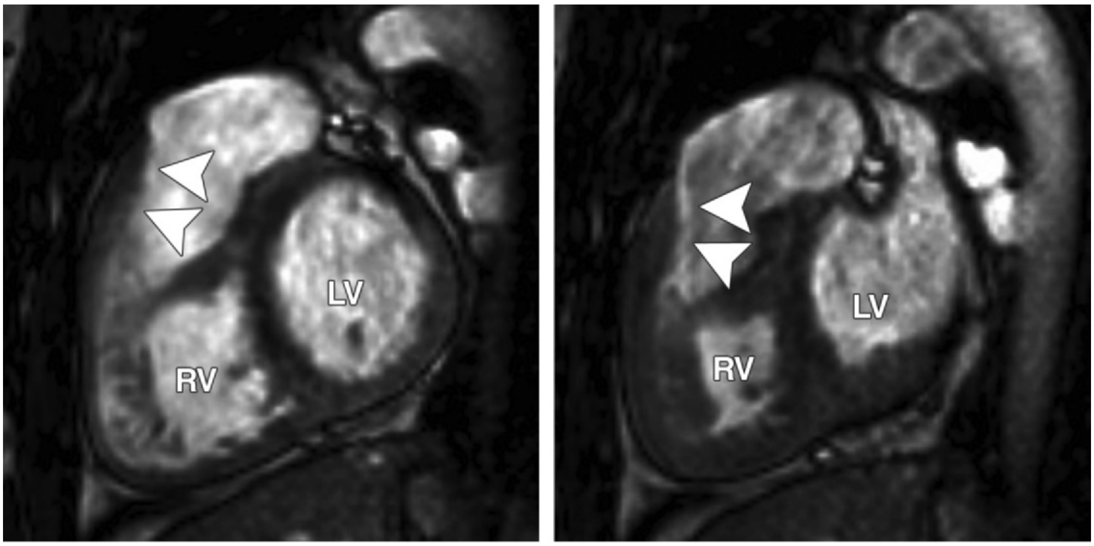

a. b.

Figure 3. Parasagittal end-diastolic **(a)** and end-systolic **(b)** SSFP cine cardiovascular MR images show normal myocardial systolic thickening at the level of the RVOT (arrowheads). *LV* = left ventricle, *RV* = right ventricle.

valve is subjected to simple commissurotomy or spared altogether in this procedure. The cardiovascular MR imaging appearance of the heart after infundibulectomy consists of an intact RVOT myocardium, with little or no evidence of fibrosis on delayed contrast material–enhanced inversion-recovery images (Fig 2). Normal RVOT contractility and a normally functioning pulmonary valve can be appreciated on steady-state free precession (SSFP) cine cardiovascular MR images (Fig 3) (14).

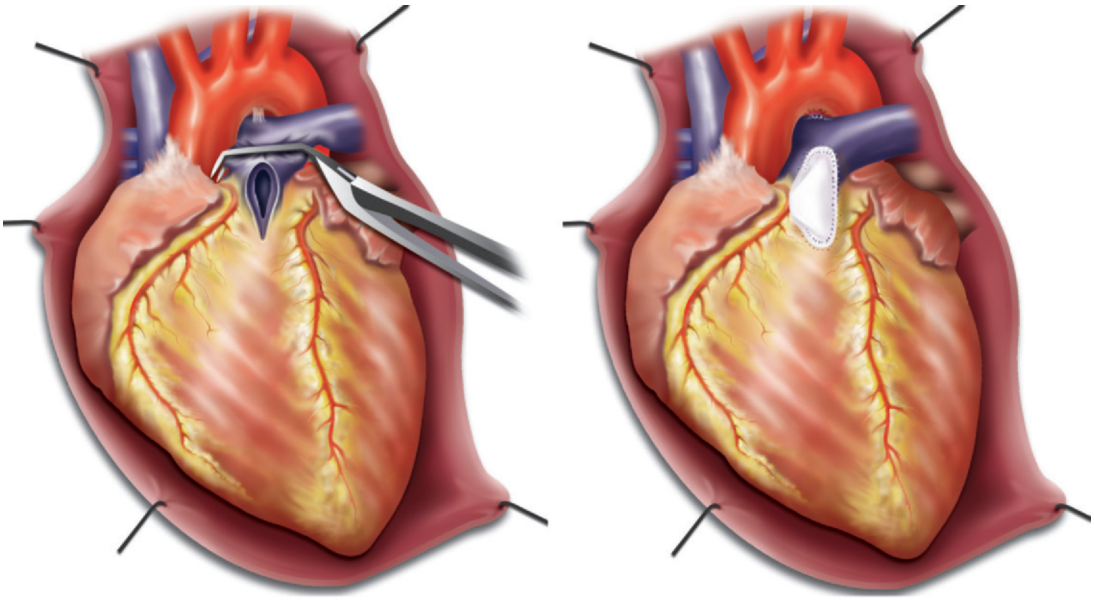

a. b.

Figure 4. Drawings illustrate transannular patch resection, consisting of transannular incision of the RVOT **(a)** and subsequent augmentation with a patch **(b)**. (Fig 4 courtesy of Joanna Culley, Haslemere, Surrey, England.)

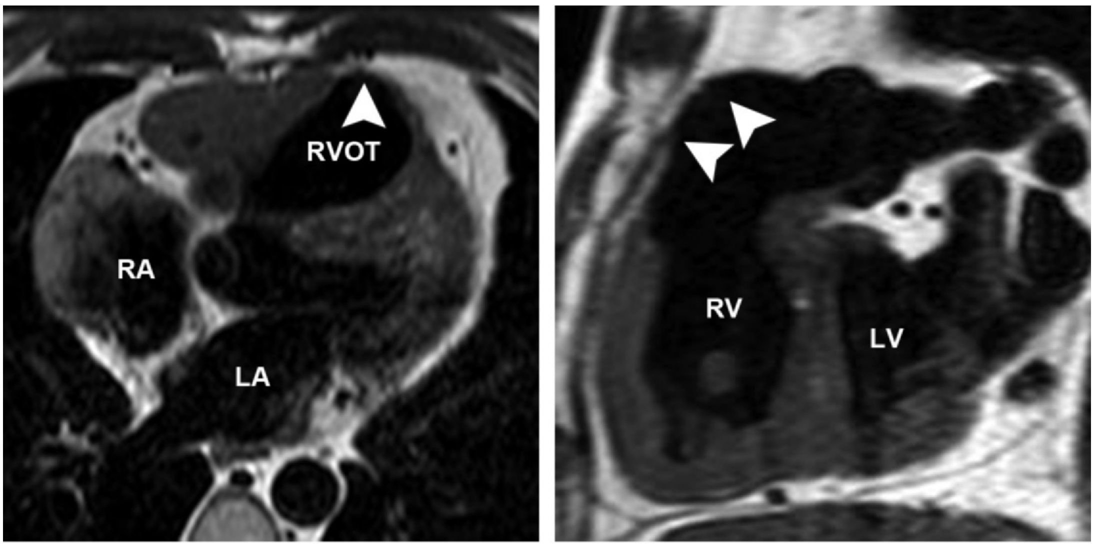

a. b.

Figure 5. Axial **(a)** and parasagittal **(b)** double-inversion-recovery spin-echo (DIR-SE) MR images show myocardial denudation of the anterior RVOT secondary to transannular patch augmentation (arrowheads). *LA* = left atrium, *LV* = left ventricle, *RA* = right atrium, *RV* = right ventricle.

Transannular patch repair is performed when there is marked stenosis of the RVOT or pulmonary annulus. The anterior wall of the RVOT is opened through the annulus of the pulmonary valve. A pericardial or synthetic (polytetrafluoroethylene [Gore-Tex; Gore, Newark, Del]) patch is then sutured to both margins of the incision, increasing the diameter of the outflow region and the main pulmonary artery (Fig 4). The patch can be extended to the branch pulmonary arteries if concomitant stenosis of these vessels is present. There is an obligatory degree of pulmonary insufficiency afterward. Cardiovascular MR images will show denudation of the anterior RVOT wall and bulging of the RVOT and main pulmonary artery, findings that represent the patch (Fig 5).

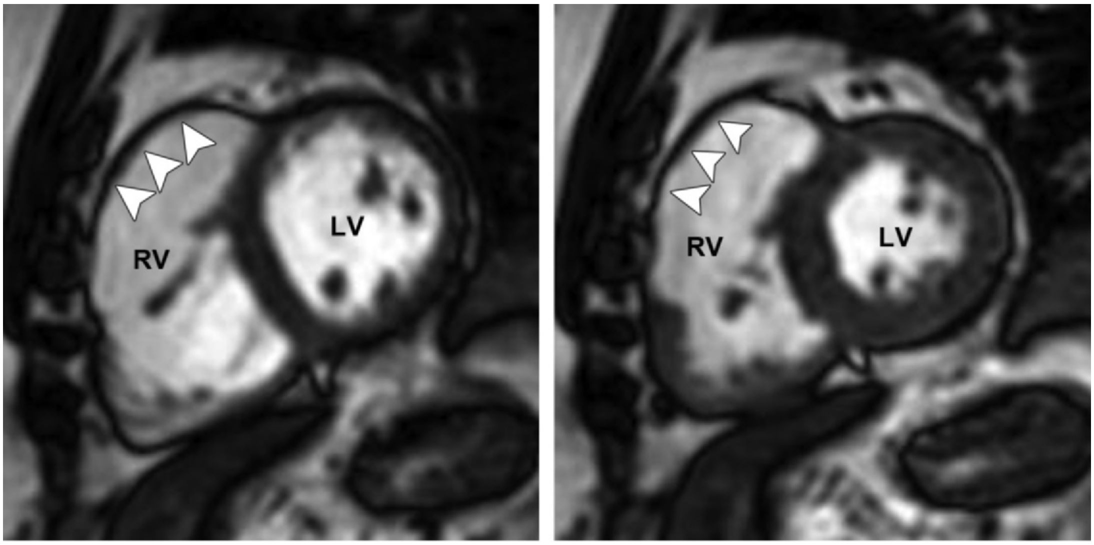

a. b.

Figure 6. End-diastolic **(a)** and end-systolic **(b)** short-axis SSFP cine cardiovascular MR images show akinesis to dyskinesis at the level of the RVOT (arrowheads). *LV* = left ventricle, *RV* = right ventricle.

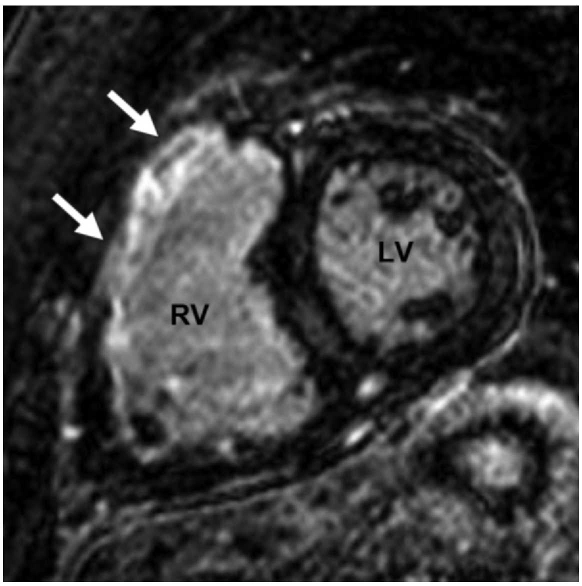

Figure 7. Delayed gadolinium-enhanced short-axis image demonstrates enhancement at the level of a transannular patch (arrows). *LV* = left ventricle, *RV* = right ventricle.

As expected, a patch does not contract during the cardiac cycle and appears as an akinetic region on SSFP cine images (Fig 6). Delayed contrast-enhanced images show enhancement in the region of the patch due to fibrotic tissue around the graft (Fig 7).

A right ventricle–pulmonary artery conduit is used in cases of atresia of the pulmonary valve or main pulmonary artery, which represents a severe variant of TOF (1). A synthetic or biologic (usually allograft or xenograft) conduit is inserted in the right ventricular anterior wall or RVOT and connected to the pulmonary arteries, which frequently need to be patched for enlargement (Fig 8). Most conduits are valved, but it is not uncommon to encounter older patients with freely regurgitant conduits due to valve degeneration. Axial images can demonstrate the attachment of the conduit to the right ventricular anterior wall and absence of myocardium around the conduit as it courses cranially and connects to the main pulmonary artery (Fig 9).

Expected Cardiovascular MR Imaging Appearance of Cardiac Problems Late after TOF Repair

The expected postoperative findings depend on the surgical procedure that was used for correction of the RVOT stenosis. For didactic purposes, we discuss separately the most common problems seen with each surgical procedure. However, most of the complications can occur with more than one type of surgical correction.

Problems Related to RVOT Resection (Infundibulectomy)

The most common late finding related to isolated RVOT resection is persistent or recurrent obstruction of the RVOT or pulmonary artery. Residual subvalvular or valvular pulmonary stenosis is seen

Teaching Point

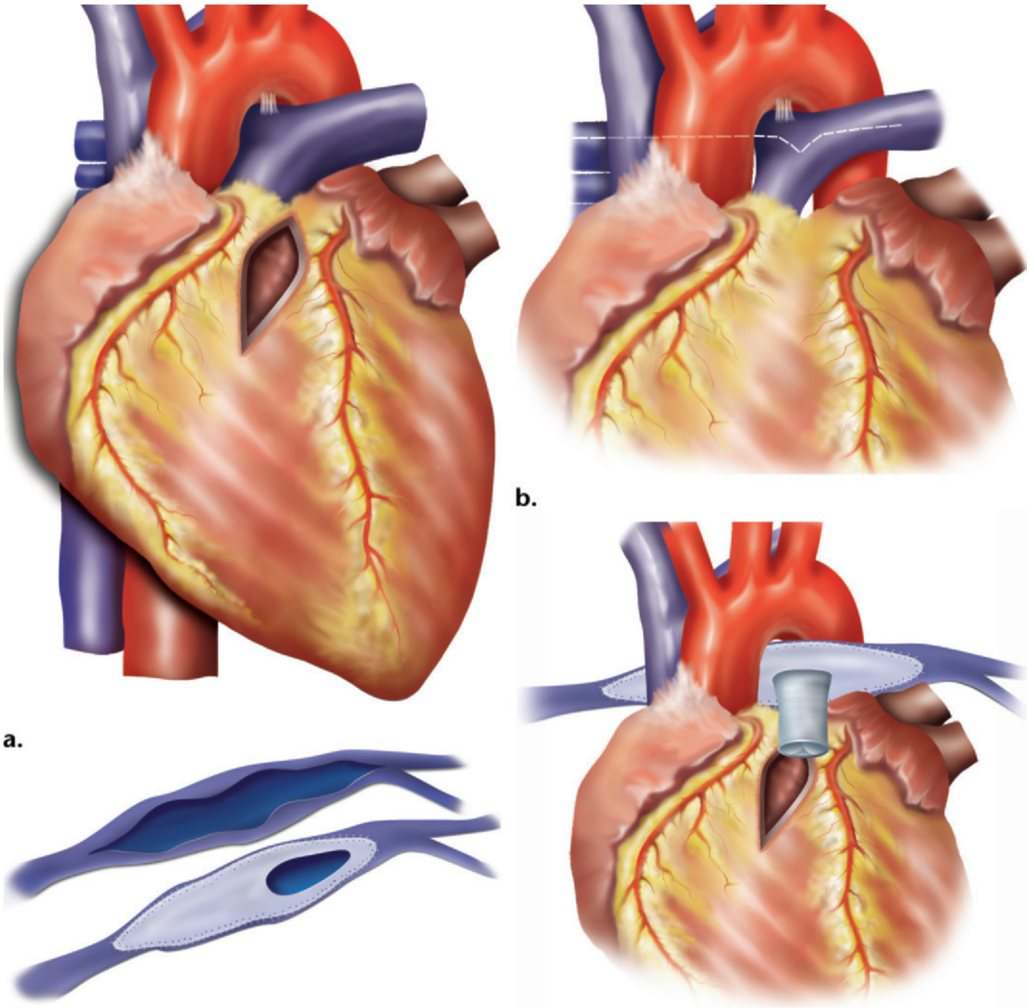

a. b. c. d.

Figure 8. Right ventricle–pulmonary artery conduit repair. **(a)** Drawing illustrates a longitudinal incision in the RVOT. **(b)** Drawing illustrates transverse incisions (dashed lines) in the anterior aspect of the right and left pulmonary arteries, including the pulmonary confluence. **(c)** Drawing illustrates anastomosis of a surgical patch to the edges of the pulmonary arterial incision. Note that an opening is made on the graft for anastomosis of the conduit. **(d)** Drawing illustrates the right ventricle–pulmonary artery conduit attached to the pulmonary arterial confluence and aligned with the RVOT incision for subsequent anastomosis. (Fig 8 courtesy of Joanna Culley, Haslemere, Surrey, England.)

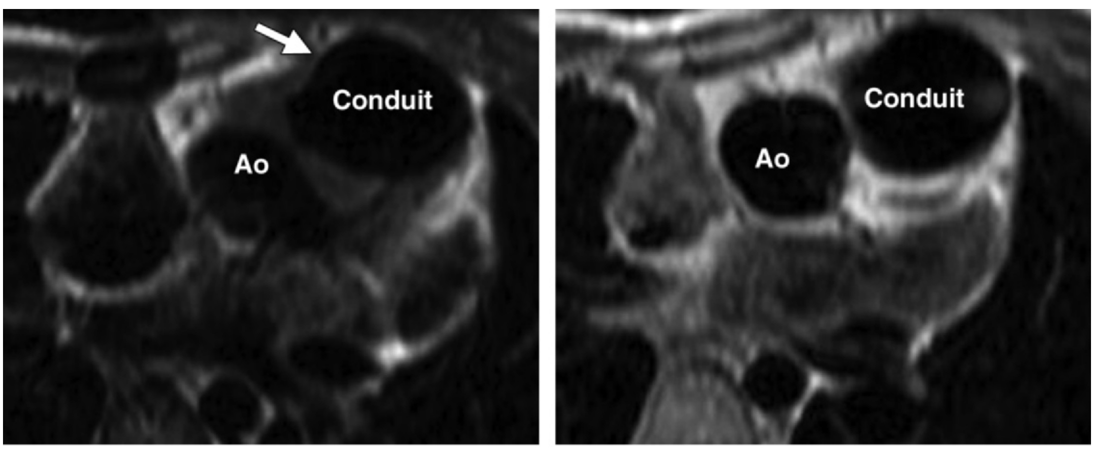

a. b.

Figure 9. **(a)** Axial DIR-SE MR image shows the attachment of a right ventricle–pulmonary artery conduit to the anterior wall of the right ventricle (arrow). *Ao* = aorta. **(b)** Axial DIR-SE MR image obtained more cranially shows the absence of myocardium around the conduit. *Ao* = aorta.

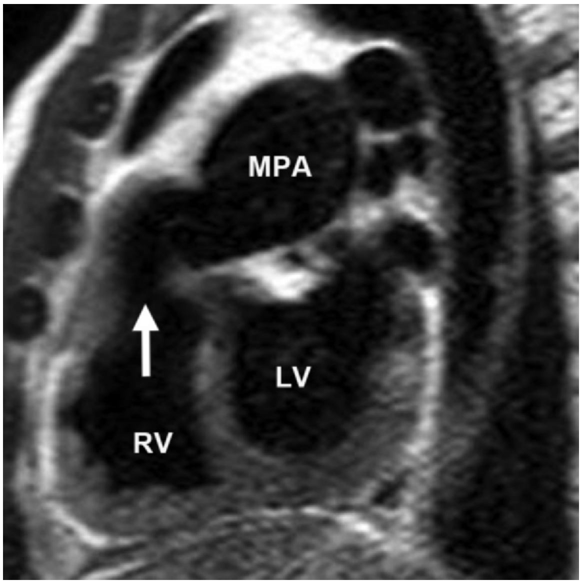

Figure 10. Parasagittal DIR-SE MR image shows residual subvalvular narrowing of the RVOT (arrow). *LV* = left ventricle, *MPA* = main pulmonary artery, *RV* = right ventricle.

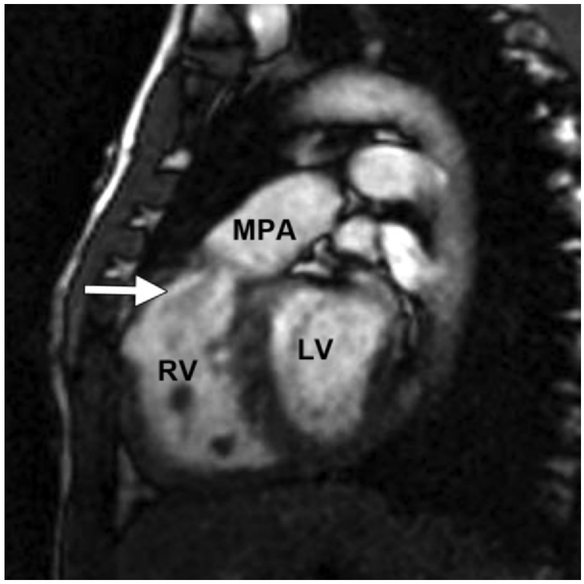

Figure 12. Parasagittal RVOT axis SSFP cine cardiovascular MR image shows a diastolic regurgitant jet across the pulmonary valve (arrow). *LV* = left ventricle, *MPA* = main pulmonary artery, *RV* = right ventricle.

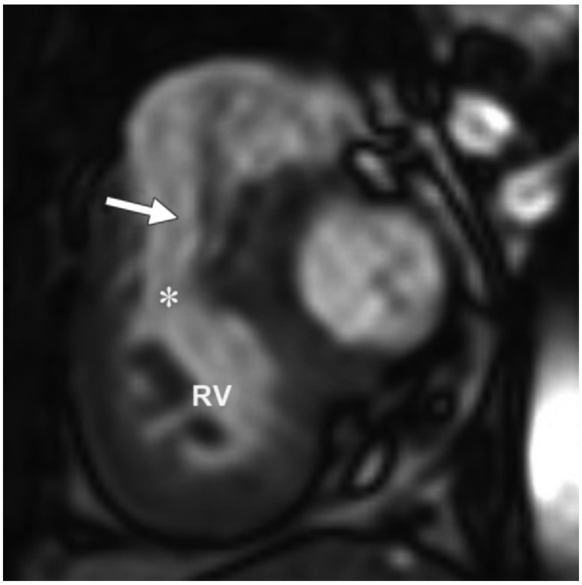

Figure 11. SSFP cine cardiovascular MR image shows residual subvalvular narrowing of the RVOT (*) and an associated systolic turbulent jet across the stenosis (arrow). *RV* = right ventricle.

in up to 5% of patients after infundibulectomy. The main clinical concern in these patients is the development of progressive right ventricular hypertrophy, which has been associated with exercise intolerance and increased risk for cardiac arrhythmias (15). Symptomatic patients typically undergo repeat surgery with further augmentation of the RVOT.

Residual RVOT stenosis can be identified on black-blood DIR-SE images, especially in the sagittal plane (Fig 10). However, the best sequence for visualizing the obstruction is the SSFP cine sequence performed in a plane parallel to the RVOT, which shows a narrowing with a resultant turbulent flow jet at the level of the stenosis (Fig 11).

Problems Related to Transannular Patch Repair

Teaching Point

The most common complications related to transannular patch augmentation of the RVOT consist of pulmonary valve insufficiency and impairment of right ventricular ejection fraction due to longstanding pulmonary regurgitation (16,17). Pulmonary regurgitation is the most common late sequela after correction of TOF. Although all three types of surgical approaches can result in pulmonary regurgitation, the use of a transannular patch is the most prone to this complication, since the valvular annulus is divided. Pulmonary regurgitation is better visualized with SSFP cine images obtained parallel to the RVOT, which show a diastolic regurgitant jet across the pulmonary valve (Fig 12).

The degree of pulmonary insufficiency after transannular patch repair varies from mild to very severe. The latter is typically seen when almost no residual valve tissue is present. Chronic pulmonary regurgitation can result in right ventricular dilatation, arrhythmias, and contractile dysfunction. Pulmonary valve replacement may be necessary to prevent or resolve these complications (3,4,6,12,18).

Another contributor to right ventricular dysfunction is the development of dyskinesis or

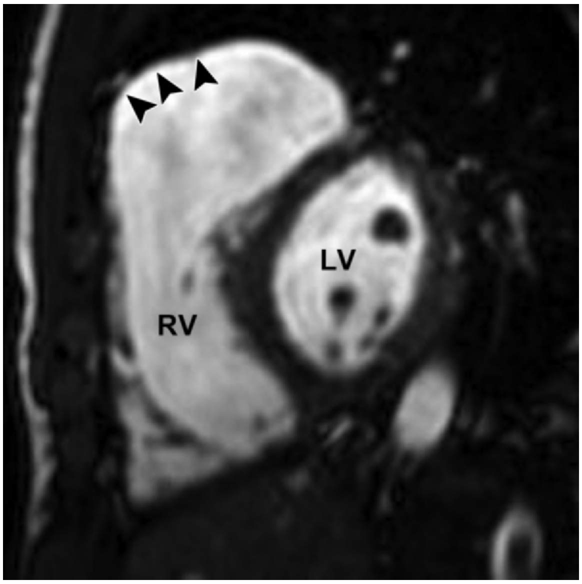

Figure 13. Short-axis SSFP cine cardiovascular MR image shows an aneurysm at the level of the RVOT (arrowheads). *LV* = left ventricle, *RV* = right ventricle.

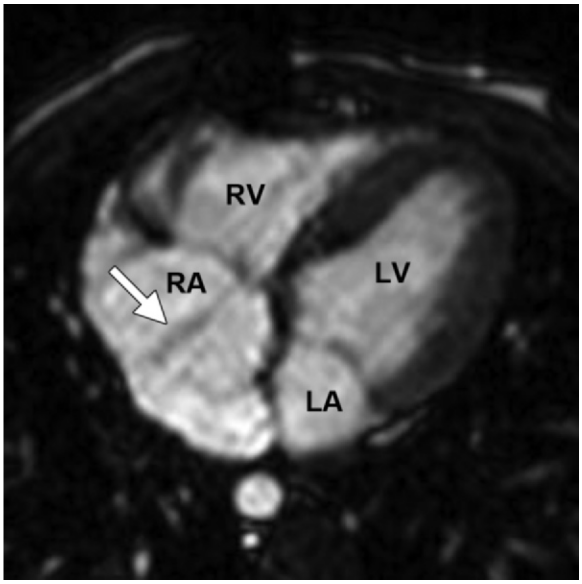

Figure 14. Four-chamber SSFP cine cardiovascular MR image shows a dilated right atrium *(RA)* and a systolic regurgitant jet across the tricuspid valve (arrow). *LA* = left atrium, *LV* = left ventricle, *RV* = right ventricle.

aneurysm of the outflow tract patch, which can be seen in approximately 50% of patients (17). RVOT dyskinesis is better identified on SSFP cine images obtained in the short-axis or RVOT planes (Fig 6). These are also the best images for evaluation of a focal or diffuse RVOT aneurysm (Fig 13). Delayed contrast-enhanced images can show extensive areas of enhancement due to both fibrotic tissue enveloping the patch and adjacent areas of fibrosis (Fig 7) (19).

The majority of patients with pulmonary regurgitation have associated tricuspid insufficiency, with a variable degree of severity. It is not known whether this tricuspid valve incompetence is due to injury during VSD closure or to tricuspid annular dilatation as a consequence of right ventricular enlargement. Right atrial enlargement seen on DIR-SE or SSFP cine images is suggestive of tricuspid regurgitation (Fig 14). SSFP cine images allow visualization of a flow jet emanating from the tricuspid valve during systole (Fig 14).

Problems Related to a Right Ventricle–Pulmonary Artery Conduit

Teaching Point

Complications of a right ventricle–pulmonary artery conduit are usually due to conduit stenosis or regurgitation of the conduit valve. Chronic degeneration and calcification is the most common cause of conduit stenosis. However, obstruction at the site of anastomosis with the pulmonary arteries can develop. Complications are seen in a high percentage of patients after conduit placement. Large follow-up studies of patients with bioprosthetic conduits have shown freedom from conduit replacement in 68%–95% of patients at 5 years and in 0%–59% at 10 years (20–22).

Degeneration of a valved conduit resulting in regurgitation is expected to occur in most conduits within 10 years of the surgical procedure (2). Most patients undergo multiple conduit replacement surgeries during their lifetime.

MR imaging can be used to assess for the presence and significance of conduit complications. Black-blood DIR-SE or SSFP cine images can demonstrate the site of conduit stenosis (Fig 15). SSFP cine images obtained at the level of the conduit can depict the narrowing of the conduit and demonstrate flow jets related to stenosis or regurgitation (Fig 16).

Problems Occurring Regardless of the Type of RVOT Augmentation Procedure

The most common abnormal findings that may be associated with all three surgical methods are recurrent or residual VSD, branch pulmonary artery stenosis or aneurysm, left pulmonary artery kinking, and left ventricular dysfunction.

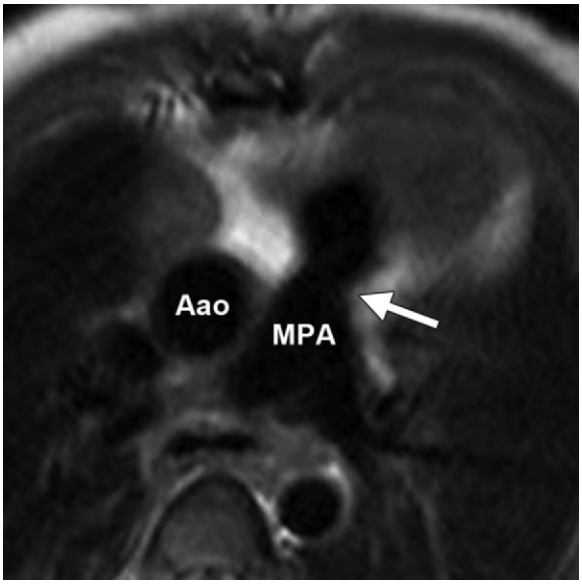

Figure 15. Axial DIR-SE MR image shows a narrowing at the level of a right ventricle–pulmonary artery conduit (arrow). *Aao* = ascending aorta, *MPA* = main pulmonary artery.

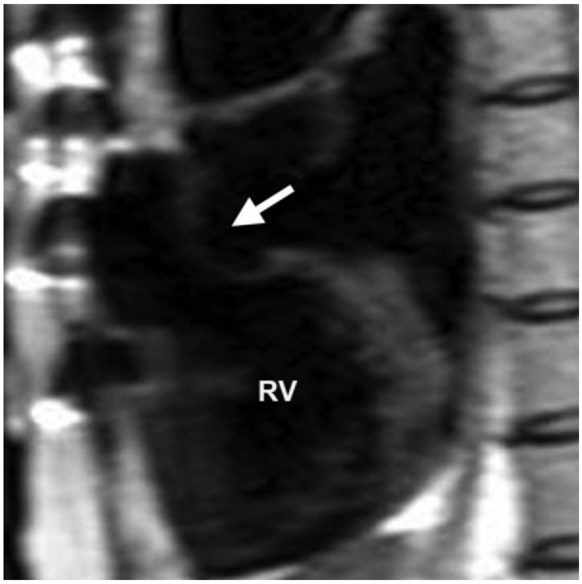

Figure 17. Sagittal DIR-SE MR image shows a VSD patch (arrow) bulging into the right ventricular *(RV)* cavity.

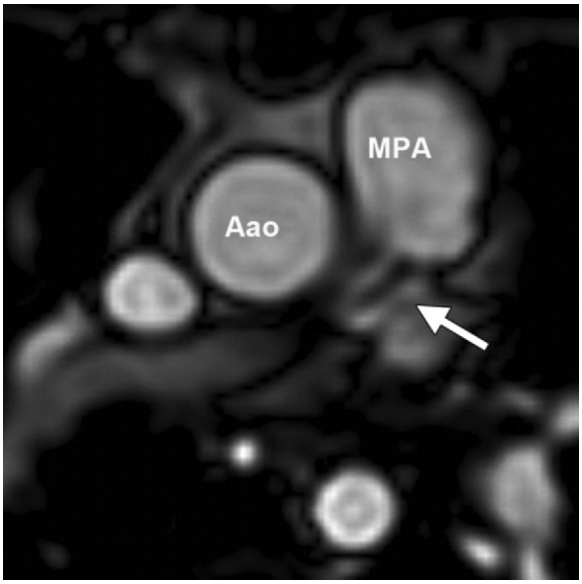

Figure 16. Axial SSFP cine cardiovascular MR image shows a turbulent flow jet at the level of a conduit stenosis (arrow). *Aao* = ascending aorta, *MPA* = main pulmonary artery.

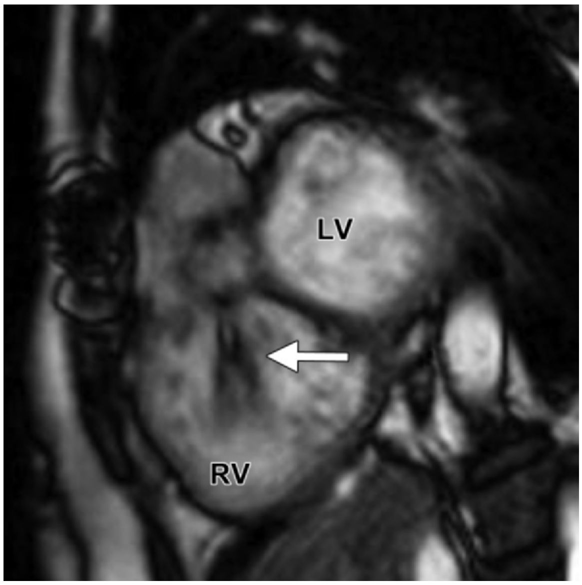

Figure 18. Short-axis SSFP cine cardiovascular MR image shows a systolic flow jet across a VSD patch to the right ventricle *(RV)* (arrow). *LV* = left ventricle.

A recurrent or residual VSD is seen is approximately 2%–5% of patients (2). This abnormality can be appreciated on black-blood images as a defect at the membranous ventricular septum. In some cases, a flaccid patch can be seen bulging into the right ventricular cavity (Fig 17). SSFP cine images can show a flow jet across the VSD patch to the right ventricle (Fig 18). The hemodynamic relevance of the VSD may be assessed by measuring the severity of the resulting shunt. Details of this technique are explained in the following section.

Branch pulmonary artery stenosis is commonly associated with native TOF. As such, it is not a true postoperative complication, although it is usually detected late postoperatively, after the main cardiac lesions have been corrected. Stenoses can be unilateral or bilateral and can

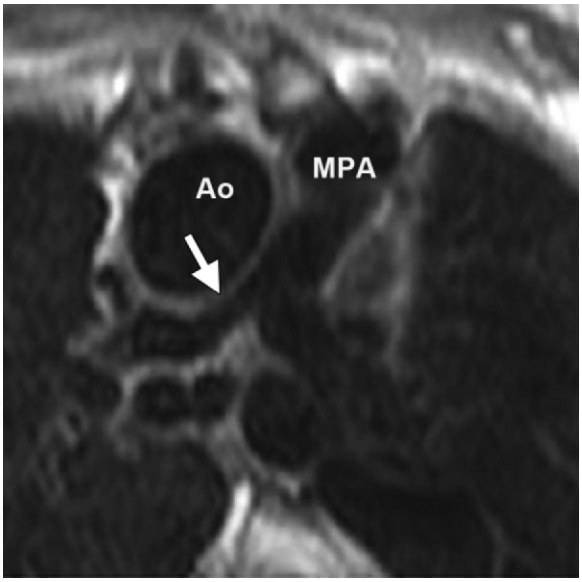

Figure 19. Axial DIR-SE MR image shows a narrowing at the level of the origin of the right pulmonary artery (arrow). *Ao* = ascending aorta, *MPA* = main pulmonary artery.

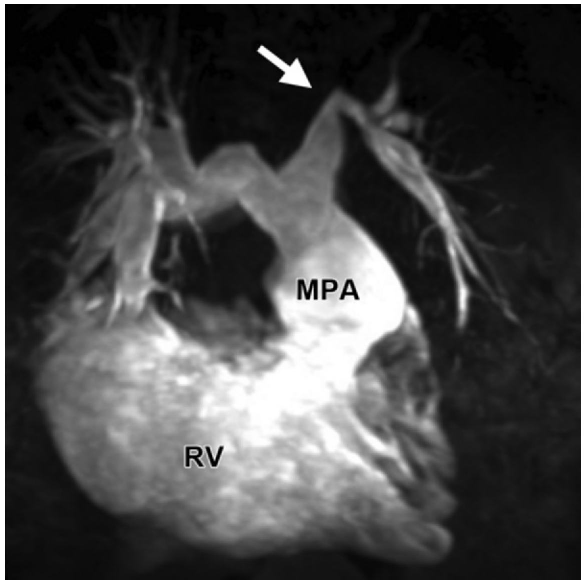

Figure 20. Contrast-enhanced maximum intensity projection MR angiographic image shows a narrowing of the left pulmonary artery (arrow). *MPA* = main pulmonary artery, *RV* = right ventricle.

involve short or long arterial segments. Aneurysms of pulmonary artery branches are usually a consequence of chronic pulmonary stenotic lesions (23). They are also classically seen with TOF associated with an absent pulmonary valve. Axial DIR-SE images can demonstrate the abnormalities in the majority of cases (Fig 19). Contrast-enhanced three-dimensional fast-field-echo MR angiography can be performed for better evaluation of branch pulmonary artery stenosis, especially when small-caliber vessels are affected in pediatric patients (Fig 20).

Kinking of the left pulmonary artery has been described in patients with a right aortic arch and severe enlargement of the RVOT or main pulmonary artery. It consists of a functional stenosis of the proximal left pulmonary artery due to an enlarged RVOT that elongates cranially and rotates to the left, since its motion is limited by the right aortic arch (19). Both DIR-SE and SSFP cine images can demonstrate an acute angle in the origin of the left pulmonary artery associated with an enlarged RVOT and right aortic arch (Fig 21).

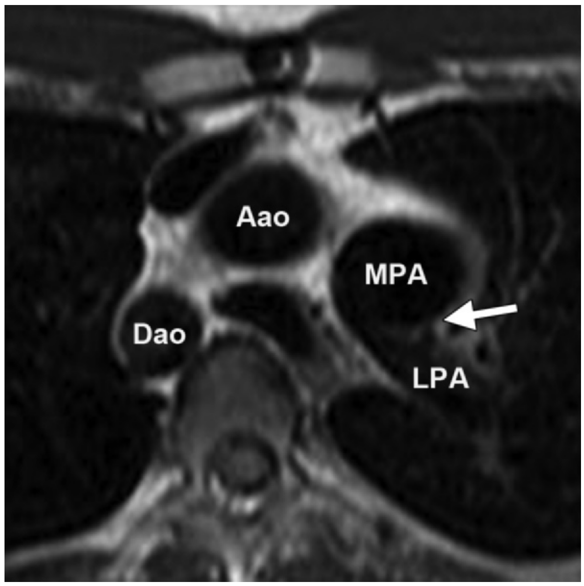

Figure 21. Axial DIR-SE MR image shows kinking of the left pulmonary artery *(LPA)* (arrow). Note the right-sided ascending aorta *(Aao)* and descending aorta *(Dao)*. *MPA* = main pulmonary artery.

Left ventricular dysfunction can be seen late after TOF repair and is an important predictor of poor outcomes in affected patients. The development of left ventricular dysfunction is likely related to poor ventriculo-ventricular interaction in patients with regional and global right ventricular dysfunction (17,24). Cardiovascular MR imaging studies performed with the tagging technique have demonstrated early abnormalities of left ventricular strain in patients with repaired TOF who still have a preserved left ventricular ejection fraction, which establishes cardiovascular MR imaging as

Suggested Cardiovascular MR Imaging Protocol for Assessment of Repaired TOF

Sequence	Plane	TR/TE (msec)	FA (°)	FOV (mm)*	ST/Gap (mm)	Matrix Size	NSA	Comments
DIR-SE T1W	Axial	Min/42	16	320 (60)	3/0.5	256/160–512	2	Breath hold
Single-dose GE	. . .	. . .	. . .	. . .	. . .	. . .	. . .	0.05 mmol/kg
Cine SSFP	Short-axis, RVOT plane	Min–3.1 /1.55	70	340	8/0	144/256	1	Breath hold
VEC MR	MPA, RVOT plane, RPA/LPA	Min–9.1 /5.7	15	300 (50)	5†	96/128–256		Above PV (MPA), before branching (RPA/LPA)
IR TFE	Short-axis, RVOT plane	Min/2	15	260 (70)	10/25	192/192–256	1	Fat saturation, navigator
3D FFE MRA	Coronal	Min5.1 /1.43	40	400	1.5†	160/400–512	1	Breath hold

Note.—FA = flip angle, FOV = field of view, GE = gadolinium-enhanced, IR TFE = inversion-recovery turbo field-echo, LPA = left pulmonary artery, Min = minimum, MPA = main pulmonary artery, NSA = number of signals acquired, PV = pulmonary valve, RPA = right pulmonary artery, ST = section thickness, TE = echo time, 3D FFE MRA = three-dimensional fast-field-echo MR angiographic, T1W = T1-weighted, TR = repetition time.

*Numbers in parentheses indicate percentage of reconstruction.

†Only one section acquired.

a possible tool for the detection of subclinical left ventricular dysfunction in these patients (25).

Another possible (albeit rare) complication after TOF repair is infarction of the right ventricular free wall due to vascular injury during surgery related to a coronary artery with an anomalous epicardial course (26). The most common anomalous coronary artery course seen in TOF is the prepulmonary course, which poses significant surgical challenges for transannular patch repair and right ventricle–pulmonary artery conduit placement (27). Injury to a coronary artery during surgical correction of TOF should be suspected in patients with severe left ventricular dysfunction and delayed enhancement following a coronary flow distribution.

Cardiovascular MR Imaging Methods for Evaluation of the Functional and Hemodynamic Severity of Complications

Although morphologic characterization of the heart and great vessels is very important in the clinical evaluation of a patient with corrected TOF, functional assessment is needed for guiding medical and surgical intervention. Functional assessment of postoperative complications of TOF is primarily based on two cardiovascular MR imaging techniques: *(a)* flow quantification with velocity-encoded cine (VEC) cardiovascular MR imaging, and *(b)* volumetric quantification with cine MR imaging. The general principles and main applications of these techniques in patients with repaired TOF are discussed in the following sections.

Cardiac MR imaging is ideally performed with a cardiac coil. The use of parallel imaging is strongly advised for achieving high temporal resolution and minimizing cardiac motion artifacts. The Table shows a suggested cardiovascular MR imaging protocol for the evaluation of patients after repair of TOF. It is important to recognize that imaging sequences and planes should be tailored to address specific clinical questions.

VEC MR Imaging

Flow Quantification.—VEC MR imaging has been shown to be an accurate method for the noninvasive quantification of blood flow (28). A phase-contrast technique based on the principle that protons in motion change phase angle in proportion to velocity, VEC MR imaging makes use of a bipolar gradient to phase encode the velocity of flow. The technique creates two imaging sets: one by subtracting the signal intensity created by stationary spins from that created by moving spins (phase image), and the other by combining the signal intensities created by stationary and moving spins (magnitude image). VEC MR imaging segments the cardiac cycle into multiple time-resolved images, allowing acquisition of multiple gated images of circulating blood flow in the heart and great vessels. VEC MR images are analyzed by manually outlining a region of interest around the main pulmonary artery on the magnitude and phase images. The region of interest provides a cross-sectional area on the magnitude image and average velocity on the phase image. The product of these two measurements is equal to instantaneous blood flow. A flow-versus-time curve can be obtained for an average cardiac cycle. For the assessment of complications after TOF repair, the main applications of VEC MR imaging include quantitative assessment of pulmonary regurgitation, differential pulmonary blood flow, and cardiac shunting, as well as assessment of the pressure gradient through an obstruction (8,11,13,29–32).

Estimation of Residual Pulmonary Stenosis.— VEC MR imaging can be used for assessment of a residual RVOT stenosis. To determine the severity of the stenosis, VEC MR imaging is performed in a plane parallel to the direction of blood flow in the RVOT to identify the maximum-velocity jet distal to the stenosis. Peak velocity can be obtained with this sequence. With use of the modified Bernoulli equation, it is possible to estimate the pressure gradient through the stenosis:

$$G_p = 4(V_p^2),$$

where G_p = peak gradient and V_p = peak velocity. Alternatively, a VEC MR imaging sequence can be performed perpendicular to the flow jet seen on the image obtained parallel to the RVOT for a more precise determination of peak velocity.

The accuracy of VEC MR imaging for the assessment of RVOT stenosis is inferior to that of Doppler echocardiography. Because VEC MR imaging does not have the real-time imaging capabilities of echocardiography, the peak velocity, and consequently the peak pressure gradient, are typically underestimated.

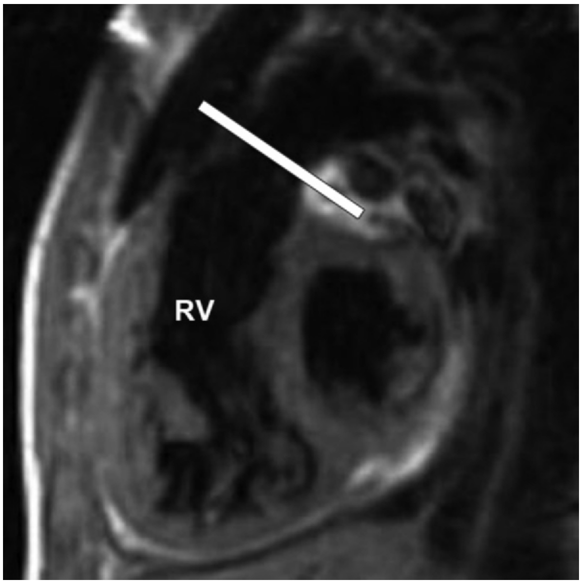

Figure 22. Image shows the optimal plane (white line) for the acquisition of VEC cardiovascular MR images at the level of the main pulmonary artery. *RV* = right ventricle.

Quantification of Valvular Regurgitation.— Cardiovascular MR imaging is the most accurate and reproducible method for quantification of pulmonary regurgitation (33,34) To calculate this value, VEC MR imaging is performed in a plane perpendicular to the direction of blood flow approximately 1 cm above the pulmonary valve (Fig 22). Measurement of forward and backward flow across the pulmonary valve allows calculation of the regurgitant fraction, which determines the severity of valvular incompetence. Pulmonary regurgitation is defined as mild if the regurgitant fraction is less than 20%, moderate if it is between 20% and 40%, and severe if it is higher than 40%.

VEC MR imaging is not accurate for the measurement of direct quantification of flow at the level of the atrioventricular valves due to significant motion during the cardiac cycle. It is possible to quantify tricuspid regurgitation by combining information obtained with VEC MR imaging in the main pulmonary artery and right ventricular volumetric quantification (35). Regurgitant flow at the tricuspid valve equals

Figure 23. On an end-diastolic short-axis SSFP cine cardiovascular MR image obtained at the basilar level, the endocardial contours of the right and left ventricles have been outlined in white for purposes of volumetric analysis.

right ventricular stroke volume minus main pulmonary artery stroke volume as measured with VEC MR imaging. Tricuspid regurgitation fraction equals tricuspid regurgitation volume divided by right ventricular stroke volume.

Quantification of Pulmonary Branch Stenosis.—When branch pulmonary stenosis is being addressed, the morphologic appearance of the branch pulmonary arteries is not a good predictor of pulmonary flow to the lungs (36). VEC MR imaging allows direct quantification of blood flow to both lungs, information that is crucial for determining the hemodynamic significance of a stenosis. Differential pulmonary flow is measured with two separate acquisitions performed perpendicular to the direction of blood flow in the proximal right and left pulmonary artery branches. The normal blood flow distribution is 55% to the right lung and 45% to the left lung.

Quantification of Residual Shunting.—In cases of possible recurrent or residual VSD, VEC MR imaging is used to determine the ratio of pulmonary to systemic blood flow (Qp/Qs). In a physiologic state, with no cardiac shunts, Qp/Qs should equal 1. For measurement of Qp/Qs, two separate sequences are performed perpendicular to the direction of blood flow in the main pulmonary artery and ascending aorta, approximately 1 cm above the respective valves. Net flow in the main pulmonary artery (Qp) is then divided by net flow in the ascending aorta (Qs). A Qp/Qs ratio higher than 1.5 is considered hemodynamically significant and generally requires surgical intervention (34,37).

Volumetric Quantification with Cardiovascular SSFP Cine MR Imaging.

For measurement of the volume of the cardiac chambers, SSFP cine images are obtained in the short-axis plane through the entire heart. For each section, 16–40 frames can be acquired over an average cardiac cycle. By manually outlining the endocardial contour of the right and left ventricles on the end-diastolic and end-systolic frames, it is possible to calculate the volumes of the chambers for each section. For better accuracy and reproducibility of the volumetric measurements, the endocardial contour should not include the papillary muscle as part of the ventricular wall (Fig 23). The volume of an entire chamber can be calculated by adding the volumes of the chamber for each section. On the basis of this technique, stroke volume can be calculated by subtracting end-systolic volume from end-diastolic volume, and ejection fraction can be calculated by dividing stroke volume by end-diastolic volume (14). Semiautomatic software for volumetric quantification is available with most cardiac MR imaging postprocessing packages.

The major application of volumetric quantification in patients with repaired TOF is to assess ventricular function, especially that of the right ventricle. Some patients with chronic pulmonary regurgitation and, consequently, an enlarged right ventricle are expected to develop right ventricular dysfunction. Early detection of this abnormality is important for determining the need for pulmonary valve replacement. In patients with pulmonary regurgitation, calculation of ejection fraction is complicated by the fact that the regurgitant volume is included in the stroke volume. An alternative indicator of right ventricular function in these patients is the effective ejection fraction, which takes into account the pulmonary regurgitation volume. The effective ejection fraction is measured by subtracting the regurgitant volume from the stroke volume and dividing the result by the end-diastolic volume.

Cine cardiovascular MR images can also be used to assess right ventricular wall motion abnormalities. By outlining the endocardial contour of the right ventricle on the end-diastolic and end-systolic frames, it is possible to track the wall motion. Quantification of the wall motion during the cardiac cycle is usually performed for multiple segments of the right ventricle and is expressed in millimeters per cycle. Tagging sequences can also be used to detect regional right ventricular wall motion abnormalities (38).

Cardiovascular MR Imaging for Prognosis and Assessment of the Need for Repeat Surgery after TOF Repair

The role of cardiovascular MR imaging in the prognostic evaluation of patients with repaired TOF has increased in recent years. One of the most important prognostic features that can be detected and quantified with cardiovascular MR imaging is myocardial fibrosis, which is characterized by areas of late enhancement on gadolinium-enhanced images. It has been shown that the presence and extent of delayed enhancement is predictive of the risk of cardiac arrhythmias and sudden death in these patients. Delayed enhancement is characteristically seen in the anterior aspect of the RVOT in patients who underwent transannular patch repair. However, recent studies have shown that the fibrotic changes can also involve the right ventricular free wall and even the left ventricular myocardium (39).

Another important prognostic indicator in patients with repaired TOF is the presence of left ventricular systolic dysfunction. Decreased left ventricular ejection fraction is associated with worse clinical outcomes in these patients, including death, sustained ventricular tachycardia, and an increase in New York Heart Association class (7). An association between left ventricular dysfunction on the one hand, and severity of pulmonary insufficiency and right ventricular dilatation on the other, has also been demonstrated (40).

Multiple studies have been conducted to determine the clinical and MR imaging parameters that could help decide the best timing for pulmonary valve replacement (41,42). In deciding when to perform surgery, one must take into account the reversibility of right ventricular dysfunction and the need for multiple valve replacement surgeries during the patient's lifetime. It has been demonstrated that patients with a decreased right ventricular ejection fraction and a right ventricular end-diastolic volume index greater than 165 mL/m^2 have worse functional recovery of the right ventricle after pulmonary valve replacement than patients with a lower right ventricular end-diastolic volume index (43). Oosterhof et al (12) demonstrated that use of an end-diastolic volume index greater than 160 mL/m^2 as a cut-off point had a sensitivity of 55% and a specificity of 92% for right ventricular function normalization after pulmonary valve replacement. It has also been shown that patients with a right ventricular end-diastolic volume index greater than 170 mL/m^2 do not experience normal right ventricular function after pulmonary valve replacement (41).

In recent years, transcatheter pulmonary valve replacement (Melody valve; Medtronic, Minneapolis, Minn) has emerged as a safe and less invasive approach after TOF repair in patients with pulmonary regurgitation or residual stenosis. A recent multicenter trial reported significant improvement in pulmonary regurgitation or stenosis after placement of this valve, with a low rate of short- and midterm valve complications (44). The size of the pulmonary valve annulus is very useful information when patients are being considered for transcatheter pulmonary valve implantation. The largest available Melody valve (Medtronic) measures 22 mm in diameter, precluding transcatheter valve replacement in patients with a wider annulus.

Advantages and Disadvantages of Cardiovascular MR Imaging and Echocardiography

Although echocardiography remains the imaging modality of choice for initial evaluation of ventricular volumes and contractility in most clinical scenarios, its use in patients with repaired TOF may be limited when significant right ventricular enlargement is present (10,45). It has been shown that MR imaging has a higher accuracy than echocardiography for the assessment of right ventricular volumes and function, particularly in patients with increased right ventricular volumes (45).

As previously discussed, precise volumetric and functional analysis of the right ventricle is crucial for decisions regarding timing of pulmonary valve replacement in this patient population. In addition, MR imaging provides a more accurate quantification of pulmonary regurgitation fraction, and it is superior to echocardiography in delineating pulmonary branch anatomy and right ventricle–

pulmonary artery conduit anatomy (13,28). The ability to delineate the cardiothoracic structures three dimensionally allows precise assessment of the spatial relationship of the heart and great vessels with the sternum, information that can be very useful for surgical planning. Three-dimensional depiction of the anatomy is particularly relevant when there is anatomic distortion due to prior surgical interventions.

Echocardiography is still an important adjunct method for the evaluation of patients with repaired TOF. The main advantages of echocardiography over cardiac MR imaging are its lower cost and wider availability. Moreover, echocardiography provides a more precise assessment of the pressure gradient across a residual pulmonary stenosis compared with cardiovascular MR imaging (46).

Conclusion

Cardiovascular MR imaging is an important tool for the follow-up of patients with repaired TOF. This imaging approach should be guided by the surgical repair procedure used and the complications that are expected. Knowledge of the most common postoperative complications and their cardiovascular MR imaging appearances is essential for good radiology practice in this clinical setting.

***Disclosures of Conflicts of Interest*.—C.B.H.:** *Related financial activities:* none. *Other financial activities:* royalties from Lippincott. **K.G.O.:** *Related financial activities:* recipient of the ARRS scholar award. *Other financial activities:* none. **S.M.:** *Related financial activities:* grant from the Swiss National Science Foundation. *Other financial activities:* none.

References

1. Murphy JG, Gersh BJ, Mair DD, et al. Long-term outcome in patients undergoing surgical repair of tetralogy of Fallot. N Engl J Med 1993;329(9):593–599.
2. Oechslin EN, Harrison DA, Harris L, et al. Reoperation in adults with repair of tetralogy of Fallot: indications and outcomes. J Thorac Cardiovasc Surg 1999;118(2):245–251.
3. Bouzas B, Kilner PJ, Gatzoulis MA. Pulmonary regurgitation: not a benign lesion. Eur Heart J 2005;26(5):433–439.
4. Bove EL, Kavey RE, Byrum CJ, Sondheimer HM, Blackman MS, Thomas FD. Improved right ventricular function following late pulmonary valve replacement for residual pulmonary insufficiency or stenosis. J Thorac Cardiovasc Surg 1985;90(1):50–55.
5. Carvalho JS, Shinebourne EA, Busst C, Rigby ML, Redington AN. Exercise capacity after complete repair of tetralogy of Fallot: deleterious effects of residual pulmonary regurgitation. Br Heart J 1992;67(6):470–473.
6. Gatzoulis MA, Balaji S, Webber SA, et al. Risk factors for arrhythmia and sudden cardiac death late after repair of tetralogy of Fallot: a multicentre study. Lancet 2000;356(9234):975–981.
7. Knauth AL, Gauvreau K, Powell AJ, et al. Ventricular size and function assessed by cardiac MRI predict major adverse clinical outcomes late after tetralogy of Fallot repair. Heart 2008;94(2):211–216.
8. Knauth Meadows A, Ordovas K, Higgins CB, Reddy GP. Magnetic resonance imaging in the adult with congenital heart disease. Semin Roentgenol 2008;43(3):246–258.
9. Meadows J, Powell AJ, Geva T, Dorfman A, Gauvreau K, Rhodes J. Cardiac magnetic resonance imaging correlates of exercise capacity in patients with surgically repaired tetralogy of Fallot. Am J Cardiol 2007;100(9):1446–1450.
10. Niezen RA, Helbing WA, van der Wall EE, van der Geest RJ, Rebergen SA, de Roos A. Biventricular systolic function and mass studied with MR imaging in children with pulmonary regurgitation after repair for tetralogy of Fallot. Radiology 1996;201(1):135–140.
11. Norton KI, Tong C, Glass RB, Nielsen JC. Cardiac MR imaging assessment following tetralogy of Fallot repair. RadioGraphics 2006;26(1):197–211.
12. Oosterhof T, van Straten A, Vliegen HW, et al. Preoperative thresholds for pulmonary valve replacement in patients with corrected tetralogy of Fallot using cardiovascular magnetic resonance. Circulation 2007;116(5):545–551.
13. Oosterhof T, Mulder BJ, Vliegen HW, de Roos A. Cardiovascular magnetic resonance in the follow-up of patients with corrected tetralogy of Fallot: a review. Am Heart J 2006;151(2):265–272.
14. Sarwar A, Shapiro MD, Abbara S, Cury RC. Cardiac magnetic resonance imaging for the evaluation of ventricular function. Semin Roentgenol 2008;43(3):183–192.
15. Rhodes JF, Hijazi ZM, Sommer RJ. Pathophysiology of congenital heart disease in the adult. II. Simple obstructive lesions. Circulation 2008;117(9):1228–1237.
16. d'Udekem Y, Rubay J, Shango-Lody P, et al. Late homograft valve insertion after transannular patch repair of tetralogy of Fallot. J Heart Valve Dis 1998;7(4):450–454.
17. Davlouros PA, Kilner PJ, Hornung TS, et al. Right ventricular function in adults with repaired tetralogy of Fallot assessed with cardiovascular magnetic resonance imaging: detrimental role of right ventricular outflow aneurysms or akinesia and adverse right-to-left ventricular interaction. J Am Coll Cardiol 2002;40(11):2044–2052.
18. Oosterhof T, Meijboom FJ, Vliegen HW, et al. Long-term follow-up of homograft function after pulmonary valve replacement in patients with tetralogy of Fallot. Eur Heart J 2006;27(12):1478–1484.
19. Oosterhof T, Mulder BJ, Vliegen HW, de Roos A. Corrected tetralogy of Fallot: delayed enhancement in right ventricular outflow tract. Radiology 2005;237(3):868–871.
20. Jonas RA, Freed MD, Mayer JE Jr, Castaneda AR. Long-term follow-up of patients with synthetic right heart conduits. Circulation 1985;72(3 pt 2):II77–II83.
21. McGoon DC, Danielson GK, Puga FJ, Ritter DG, Mair DD, Ilstrup DM. Late results after extracardiac conduit repair for congenital cardiac defects. Am J Cardiol 1982;49(7):1741–1749.

RadioGraphics

22. Razzouk AJ, Williams WG, Cleveland DC, et al. Surgical connections from ventricle to pulmonary artery: comparison of four types of valved implants. Circulation 1992;86(5 suppl):II154–II158.
23. Bashore TM. Adult congenital heart disease: right ventricular outflow tract lesions. Circulation 2007;115(14):1933–1947.
24. Muzzarelli S, Ordovas KG, Cannavale G, Meadows AK, Higgins CB. Tetralogy of Fallot: impact of the excursion of the interventricular septum on left ventricular systolic function and fibrosis after surgical repair. Radiology 2011;259(2):375–383.
25. Ordovas KG, Carlsson M, Lease KE, et al. Impaired regional left ventricular strain after repair of tetralogy of Fallot. J Magn Reson Imaging 2012; 35(1):79–85.
26. Bhutani AK, Koppala MM, Abraham KA, Balakrishnan KR, Desai RN. Inadvertent transection of anomalously arising left anterior descending artery during tetralogy of Fallot repair: bypass grafting with left internal mammary artery. J Thorac Cardiovasc Surg 1994;108(3):589–590.
27. White RI Jr, Frech RS, Castaneda A, Amplatz K. The nature and significance of anomalous coronary arteries in tetralogy of Fallot. Am J Roentgenol Radium Ther Nucl Med 1972;114(2):350–354.
28. Rebergen SA, Chin JG, Ottenkamp J, van der Wall EE, de Roos A. Pulmonary regurgitation in the late postoperative follow-up of tetralogy of Fallot: volumetric quantitation by nuclear magnetic resonance velocity mapping. Circulation 1993;88(5 pt 1):2257–2266.
29. Wu MT, Huang YL, Hsieh KS, et al. Influence of pulmonary regurgitation inequality on differential perfusion of the lungs in tetralogy of Fallot after repair: a phase-contrast magnetic resonance imaging and perfusion scintigraphy study. J Am Coll Cardiol 2007;49(18):1880–1886.
30. Weber OM, Higgins CB. MR evaluation of cardiovascular physiology in congenital heart disease: flow and function. J Cardiovasc Magn Reson 2006; 8(4):607–617.
31. Abd El Rahman MY, Hui W, Yigitbasi M, et al. Detection of left ventricular asynchrony in patients with right bundle branch block after repair of tetralogy of Fallot using tissue-Doppler imaging-derived strain. J Am Coll Cardiol 2005;45(6):915–921.
32. Brenner LD, Caputo GR, Mostbeck G, et al. Quantification of left to right atrial shunts with velocity-encoded cine nuclear magnetic resonance imaging. J Am Coll Cardiol 1992;20(5):1246–1250.
33. Wagner S, Auffermann W, Buser P, et al. Diagnostic accuracy and estimation of the severity of valvular regurgitation from the signal void on cine magnetic resonance images. Am Heart J 1989;118(4): 760–767.
34. Varaprasathan GA, Araoz PA, Higgins CB, Reddy GP. Quantification of flow dynamics in congenital heart disease: applications of velocity-encoded cine MR imaging. RadioGraphics 2002;22(4):895–905; discussion 905–906.
35. Cawley PJ, Maki JH, Otto CM. Cardiovascular magnetic resonance imaging for valvular heart disease: technique and validation. Circulation 2009; 119(3):468–478.
36. Ordovás KG, Tan C, Reddy GP, Weber OM, Lu Y, Higgins CB. Disparity between ratios of diameters and blood flows in central pulmonary arteries in postoperative congenital heart disease using MRI. J Magn Reson Imaging 2007;25(4):721–726.
37. Warnes CA, Williams RG, Bashore TM, et al. ACC/AHA 2008 Guidelines for the Management of Adults with Congenital Heart Disease: a report of the American College of Cardiology/American Heart Association Task Force on Practice Guidelines (writing committee to develop guidelines on the management of adults with congenital heart disease). Circulation 2008;118(23):e714–e833.
38. Youssef A, Ibrahim SH, Korosoglou G, Abraham MR, Weiss RG, Osman NF. Strain-encoding cardiovascular magnetic resonance for assessment of right-ventricular regional function. J Cardiovasc Magn Reson 2008;10:33.
39. Babu-Narayan SV, Kilner PJ, Li W, et al. Ventricular fibrosis suggested by cardiovascular magnetic resonance in adults with repaired tetralogy of fallot and its relationship to adverse markers of clinical outcome. Circulation 2006;113(3):405–413.
40. Cheung EW, Liang XC, Lam WW, Cheung YF. Impact of right ventricular dilation on left ventricular myocardial deformation in patients after surgical repair of tetralogy of Fallot. Am J Cardiol 2009; 104(9):1264–1270.
41. Therrien J, Provost Y, Merchant N, Williams W, Colman J, Webb G. Optimal timing for pulmonary valve replacement in adults after tetralogy of Fallot repair. Am J Cardiol 2005;95(6):779–782.
42. Henkens IR, van Straten A, Schalij MJ, et al. Predicting outcome of pulmonary valve replacement in adult tetralogy of Fallot patients. Ann Thorac Surg 2007;83(3):907–911.
43. Geva T. Indications and timing of pulmonary valve replacement after tetralogy of Fallot repair. Semin Thorac Cardiovasc Surg Pediatr Card Surg Annu 2006:11–22.
44. McElhinney DB, Hellenbrand WE, Zahn EM, et al. Short- and medium-term outcomes after transcatheter pulmonary valve placement in the expanded multicenter US Melody valve trial. Circulation 2010;122(5):507–516.
45. Helbing WA, Bosch HG, Maliepaard C, et al. Comparison of echocardiographic methods with magnetic resonance imaging for assessment of right ventricular function in children. Am J Cardiol 1995;76 (8):589–594.
46. Didier D, Ratib O, Lerch R, Friedli B. Detection and quantification of valvular heart disease with dynamic cardiac MR imaging. RadioGraphics 2000;20 (5):1279–1299; discussion 1299–1301.

Cardiovascular MR Imaging after Surgical Correction of Tetralogy of Fallot: Approach Based on Understanding of Surgical Procedures

Karen G. Ordovas, MD, MAS • Stefano Muzzarelli, MD • Michael D. Hope, MD • David M. Naeger, MD • Tom Karl, MD • Gautham P. Reddy, MD, MPH • Edson Marchiori, MD, PhD • Charles B. Higgins, MD

RadioGraphics 2013; 33:1037–1052 • **Published online** 10.1148/rg.334115084 • **Content Codes:** CA CH MR PD

Page 1038
Early detection and treatment of postoperative complications are important to prevent progressive loss of right ventricular function with consequent impairment of exercise capacity and increased risk of fatal arrhythmias.

Page 1041
The most common late finding related to isolated RVOT resection is persistent or recurrent obstruction of the RVOT or pulmonary artery.

Page 1043
The most common complications related to transannular patch augmentation of the RVOT consist of pulmonary valve insufficiency and impairment of right ventricular ejection fraction due to long-standing pulmonary regurgitation.

Page 1043
Pulmonary regurgitation is the most common late sequela after correction of TOF. Although all three types of surgical approaches can result in pulmonary regurgitation, the use of a transannular patch is the most prone to this complication, since the valvular annulus is divided. Pulmonary regurgitation is better visualized with SSFP cine images obtained parallel to the RVOT, which show a diastolic regurgitant jet across the pulmonary valve.

Page 1044
Complications of a right ventricle–pulmonary artery conduit are usually due to conduit stenosis or regurgitation of the conduit valve.